Pergamon

Geochimica et Cosmochimica Acta, Vol. 63, No. 11/12, pp. 1853–1863, 1999

0016-7037/99 $20.00 + .00

PII S0016-7037(99)00059-9

Oxygen fugacity dependence of Ni, Co, Mn, Cr, V, and Si partitioning between liquid metal and magnesiowüstite at 9–18 GPa and 2200°C

C. K. Gessmann, D. C. Rubie, and C. A. McCammon
Bayerisches Geoinstitut, Universität Bayreuth, D-95440 Bayreuth, Germany

(*Received May* 31, 1998; *accepted in revised form November* 8, 1998)

Abstract—The oxidation states of Ni, Co, Mn, Cr, V and Si in magnesiowüstite have been determined in metal-oxide distribution experiments using a multi anvil apparatus at 9 and 18 GPa and 2200°C as a function of oxygen fugacity. Despite limitations to control oxygen fugacity by applying conventional buffering methods in high pressure experiments, a wide range of redox-conditions (3 log bar units) has been imposed to the metal-oxide partitioning experiments by varying the Si/O ratio of the starting material. The oxygen fugacity was calculated according to the Fe-FeO equilibrium between the run products. The ability to impose different oxygen fugacities by varying the starting material is confirmed by the large variation of element partitioning coefficients obtained at constant pressure and temperature. The calculated valences at both pressures investigated are divalent for Co, Mn, V and 4+ for Si. The results for Cr (~2.5+) and Ni (~1.5+) indicate non-ideal mixing of Ni and Cr in at least one of the product phases. Because the application of 1 bar activity coefficients for Ni and Cr in metal alloys does not change these valences, non-ideal mixing in magnesiowüstite or significantly larger non-ideal mixing properties of Ni and Cr in metal alloys at high pressure are likely to be responsible for the apparent valences. Omitting such non-ideal mixing properties when extrapolating high-pressure element partitioning data may be significant. The elements Cr, V and Mn become siderophile ($D_M^{met/ox} > 1$) at 9–18 GPa and 2200°C at oxygen fugacities below IW-2.7 to IW-3.7. Considering, in addition, the influence of temperature, the depletion of Cr, Mn and V in the Earth's mantle may be due, at least partly, to siderophile behavior at high pressure and temperature. *Copyright © 1999 Elsevier Science Ltd*

1. INTRODUCTION

Investigations of the partitioning of siderophile elements in metal–oxide and metal–silicate systems are essential for interpreting the geochemistry of the Earth's mantle in terms of the processes of core formation (e.g. Ringwood, 1966; Jones and Drake, 1986; Li and Agee, 1996; Righter et al. 1997). Partitioning behavior is strongly dependent on oxygen fugacity in such systems. Therefore element partitioning must either be investigated experimentally over a wide range of oxygen fugacities or it must be possible to reliably extrapolate the results as a function of oxygen fugacity. In the latter case, knowledge of the valence states and thermodynamic mixing properties of the elements of interest is required. In addition, knowledge of valence states is essential for comparing the results of experiments performed at different oxygen fugacities. Such a comparison involves normalizing the results to a certain oxygen fugacity, for which the valence states must be known.

Although the valence states of a range of major and minor elements (siderophile to lithophile) have been studied extensively at 1 bar (e.g. Hillgren, 1991; Holzheid et al., 1994; Borisov and Palme, 1995; O'Neill et al., 1995; Ertel, 1996; Ertel et al., 1996), investigations at high pressure are rare and cover only very small ranges of redox conditions (<1 log bar unit). This is because of the technical difficulties involved in controlling oxygen fugacity in multianvil experiments as discussed below. Therefore, changes in the oxidation states of transition elements, which have been predicted to be induced by high pressure (Burns, 1993; Li et al., 1995), have not been verified experimentally for mantle materials (even though such changes would have far-reaching geochemical consequences). Although the valence states of elements such as Ni and Co are not expected to change at high pressure and temperature, this may not be the case for elements with multiple valence states such as Fe, Cr, and V.

The effects of oxygen fugacity on the partitioning behavior of Cr, V, and Mn are particularly interesting. These elements are depleted in the Earth's mantle relative to a C1-normalized composition (Ringwood, 1966) and several alternative explanations for this depletion have been discussed. (1) They were siderophile during core formation and consequently have been largely extracted from the mantle by the metal that accumulated to form the core or (2) they were lost as a consequence of high volatility during accretion. In connection with testing the first hypothesis, distribution coefficients determined for Cr, V, and Mn at mantle pressures and temperatures can indicate the conditions (e.g., oxygen fugacities) that would have been required for these elements to become siderophile.

Methods for buffering oxygen fugacity in experiments at relatively low pressures (e.g., the double capsule technique) are well established (e.g. Luth, 1993). At higher pressures and temperatures, relevant to the Earth's mantle, experiments are performed up to 26 GPa and 2800°C using the multianvil apparatus. Because of the small sample size of this apparatus, it is very difficult to control oxygen fugacity by applying conventional buffering methods, or to measure oxygen fugacity in situ by introducing an oxygen sensor into the high-pressure sample assembly. Because of these limitations, studies at high

Address reprint requests to C. K. Gessmann, Department of Earth Sciences, University of Bristol, Wills Memorial Building, Queens Road, Bristol BS8 1RJ, U.K.; E-mail: christine.gessman@bristol.ec.uk.

Table 1. Composition of the starting materials.

#	Mix 1a[a] (wt%)	Mix 2 (wt%)	Mix 4a[a] (wt%)	Mix 5a[a] (wt%)	Mix 6a[a] (wt%)	Mix 7 (wt%)
Fe	72.59	50.41	59.50	56.65	61.12	71.49
Fe_3O_4		25.19			12.41	
Ni	15.78	14.82	13.05	12.41	15.18	15.52
Co[a]	1.49[a]		1.47[a]	1.50	1.50[a]	
Mn	1.57	1.61	1.64	1.53	1.58	1.55
Cr	1.57	1.61	1.59	1.57	1.58	1.55
V			1.58	1.45		
V_2O_5	2.76	2.02			2.37	2.72
Si			1.78	6.63		3.0
SiO_2	2.17	2.24	16.99	16.34	2.19	2.13
TiO_2	2.07	2.10	2.40	1.97	2.07	2.04
Fe/Ni	4.59	4.63	4.56	4.56	4.62	4.606
Si/O	0.317	0.106	0.971	1.503	0.158	1.314

[a] Mixes 1, 4, 5 and 6 are without Co.

pressures and temperatures in which oxygen fugacity has been systematically varied over a wide range are nonexistent. It is therefore important to develop and establish techniques that enable redox conditions to be varied and oxygen fugacities to be estimated in experiments that are performed under mantle conditions.

In the present study we determine metal–magnesiowüstite distribution coefficients for Ni, Co, Mn, Cr, V, and Si at high pressures (9 and 18 GPa) and constant temperature (2200°C) as a function of oxygen fugacity. An important objective is to obtain results from high-pressure multianvil experiments over a very wide range of oxygen fugacities. From the partitioning results we calculate the valence states of Ni, Co, Mn, Cr, V, and Si in magnesiowüstite at high pressure and consider whether these valence states change with increasing pressure, as has been predicted theoretically. We use the determined valences to indicate whether or not magnesiowüstite and liquid metal solid solutions can be described by ideal mixing models at high pressures and temperatures. Finally we consider conditions at which Cr, Mn, and V would have been siderophile during core formation.

2. EXPERIMENTAL DETAILS

High-pressure experiments were performed using a 1200-tonne multianvil apparatus (Ito et al., 1984; Liebermann and Wang, 1992). The sample assembly consisted of an MgO (+5 wt% Cr_2O_3) octahedron, with an edge length of either 18 mm or 10 mm, containing a cylindrical $LaCrO_3$ heater. In the case of the 18 mm octahedron the heater had a stepped wall thickness to minimize thermal gradients (Canil, 1991; Rubie et al., 1993a). The octahedron was compressed using 32-mm cubic tungsten carbide anvils (Toshiba grade F) with truncation edge lengths of either 11 mm (18 mm octahedron) or 5 mm (10 mm octahedron). The sample capsule consisted of MgO and contained ~6 mg of starting material. Temperature was monitored with a W3%Re/W25%Re thermocouple with the thermocouple junction placed in direct contact with the end of the capsule. Pressure was calibrated using Bi phase transitions at room temperature and SiO_2 and Fe_2SiO_4 phase transformations at 1000°C and 1450°C (see Rubie et al., 1993b). The uncertainties in pressure and temperature are estimated to be ~0.5 GPa and ~40°C, respectively.

Starting materials consisted of Fe–Ni powders doped with 1–1.5 wt% of various elements (Co, Mn, Cr, V, Ti) and also varying amounts of Si which were added as either elements or oxides (Table 1). While all of the starting materials had similar Fe/Ni ratios and similar concentrations of the minor elements, the Si and O contents were varied (see Si/O ratios listed in Table 1). These compositional variations result in different redox levels and the production of varying proportions of silicate melt. Two starting mixtures (mixes 2 and 6) also included some ferric iron (added as Fe_3O_4). In two experiments (#1334 and #1342) the MgO capsule was surrounded with Re foil. In these experiments, significant amounts of Re dissolved in the liquid metal, resulting in the formation of Fe–Ni–Re alloys which equilibrated with magnesiowüstite.

In each experiment, the sample was first pressurized to the desired pressure (9–18 GPa); the temperature was then raised at ~100°C/min to the desired run temperature (2200°C), and then held there for 5–20 min (Table 2). The sample was quenched by switching off the power to the $LaCrO_3$ furnace (initial quench rate ~500°C/s) and then decompressed over a period of 10–12 hs. After completion of the experiment, the entire sample assembly was mounted in epoxy and a section through the center of the sample was polished for electron microprobe analysis. Samples were routinely analyzed using a CAMECA SX50 electron microprobe (20 keV, 50 nA, 100 s counting time for trace elements and 50–80 s counting time for major elements). Fe metal, Ni metal, Co metal, forsterite, periclase, Cr_2O_3, $MnTiO_3$, and V_2O_5 were employed as standards. The detection limits of around 50 ppm for the analyzed elements under similar analyzing conditions have been reported (Ramsden and French, 1990). However, the detection limits calculated employing the formula given by Brümmer (1977) based on the calibration data and analyzing conditions are as follows: Mg ~110 ppm, Si ~100 ppm, Ti ~90 ppm, Fe ~200 ppm, Ni ~310 ppm, Co ~200 ppm, Mn ~150 ppm, Cr ~170 ppm, V ~190 ppm.

3. THEORETICAL BACKGROUND

The partitioning of a siderophile element M between a metal and a silicate or oxide phase can be written as a general reaction:

$$\underset{\text{metal (met)}}{M} + (x/4)O_2 \quad \Leftrightarrow \quad \underset{\text{oxide (ox)}}{MO_{x/2}}, \qquad (1)$$

where M is the siderophile element and x is the valence of element M in the oxide phase. The equilibrium constant K for reaction (1) is

$$K = a^{ox}_{MO_{x/2}}/[a^{met}_{M}(fO_2)^{x/4}], \qquad (2)$$

where fO_2 is the oxygen fugacity and $aO_2 \equiv fO_2$.

The Gibbs free energy ΔG_0 for reaction (1) can be expressed as

$$\Delta G_0 = -RT \ln K = -2.303\, RT \log K, \qquad (3)$$

where R is the gas constant, T is the absolute temperature, and K is the equilibrium constant of reaction (1). The activity of a component i in phase j is given as

Table 2. Experimental conditions, calculated oxygen fugacities and the volume proportion of exsolved blobs in quenched metal. The temperature of all experiments was 2200°C.

Experiment #	Pressure (GPa)	Time (min)	Starting material Mix #	Calculated log 10 oxygen fugacity[a]	Calculated log 10 oxygen fugacity[b]	Volume % of blobs
1186[d]	9	16	1	−2.09	−1.63	1.95
1194	9	16	2	−1.30	−0.95	7.13
1200[d]	9	16	4	−2.71	−2.19	0.32
1203	9	16	5	−3.51	−2.98	0.72
1210	9	16	6	−1.52	−1.11	5.11
1218	9	16	7	−2.85	−2.32	1.01
1316	9	16	5a	−3.54	−3.94	0.28
1352[d]	9	16	6a	−1.50	−1.15	5.72
1371[d]	9	4	6a	−1.45	−1.09	5.98
1383[d]	9	8	6a	−1.53	−1.14	6.15
1273	18	7	4	−2.32	−1.85	0.44
1275	18	15	1	−2.24	−1.64	1.22
1285	18	16	2	−1.09	−0.80	4.46
1320	18	10	5a	−3.11	−2.55	0.11
1334[c]	18	10	4a	−2.67	−2.07	0
1342[c]	18	8	6a	−1.33	−0.90	0

[a] Oxygen fugacity calculated relative to the Fe–FeO equilibrium assuming activity coefficients being unity; for details see text.
[b] Oxygen fugacity calculated relative to the Fe–FeO equilibrium employing 1 bar activity coefficients reported by Screcec et al. (1987) and Rammensee and Fraser (1981); for details see text.
[c] Experiment performed with a Re–foil capsule sourrounding the MgO capsule.
[d] Results from Gessmann and Rubie, 1998.

$$a_i^j = X_i^j \gamma_i^j \quad , \tag{4}$$

where X_i^j is the mole fraction of component i in phase j and γ_i^j is the activity coefficient. Combining Eqns 2, 3, and 4 then gives:

$$\Delta G_0/2.303\,RT = -\log K = \log X_M \gamma_M^{met} + (x/4)\log fO_2 - \log X_{MO_{x/2}} \gamma_{MO_{x/2}}^{ox} \tag{5}$$

and rearrangement yields:

$$\log (X_M^{met}/X_{MO_{x/2}}^{ox}) = -\log K - (x/4)\log fO_2 - \log \gamma_M^{met} + \log \gamma_{MO_{x/2}}^{ox} \tag{6}$$

The distribution coefficient ($D_M^{met/ox} = c_M^{met}/c_M^{ox}$; wt% basis) is related to Eqn 6 by conversion factors k and k':

$$\log D_M^{met/ox} = \log k(X_M^{met}/X_{MO_{x/2}}^{ox}) = -(x/4)\log fO_2 - \log K - \log \gamma_M^{met} + \log \gamma_{MO_{x/2}}^{ox} + k'. \tag{7}$$

Equation 7 relates the logarithm of the distribution coefficient linearly to the oxygen fugacity with the constants log K, log γ_M, log $\gamma_{MO_{x/2}}$, and k'. The slope $(-x/4)$ gives the valence x of element M in the oxide phase.

It should be noted that values of γ_M^{met} and $\gamma_{MO_{x/2}}^{ox}$ are constant if the dilution of element M is infinite in the respective phases (i.e., Henry's law is fulfilled), which may not always be the case in the present experiments. Possible deviations from constant activity coefficients will be discussed in the following section. When activity coefficients are composition-dependent their values must be known in order to determine valences using the above equations. However, activity coefficients which are relevant to the present study have so far only been determined at 1 bar and relatively low temperatures.

It is clear that Eqn 7 can only be used to determine the valence of element M if the oxygen fugacity is known. It is difficult to control oxygen fugacity in multianvil high-pressure experiments because the sample volumes are generally too small to allow buffering techniques (e.g., double capsule technique) to be employed. Alternatively, the presence of a metal M in equilibrium with a corresponding $MO_{x/2}$-bearing phase in high-pressure experiments enables redox conditions, relative to the respective M-$MO_{x/2}$ buffer curve under experimental conditions, to be constrained. In the present experiments equilibrium between Fe-rich metal and magnesiowüstite can be described by the reaction:

$$\underset{\text{metal}}{Fe} + (x/4)O_2 \Leftrightarrow \underset{\text{magnesiowüstite}}{Fe^{x+}O_{x/2}} \quad . \tag{8}$$

The equilibrium constant for this reaction with $x = 2$ (for FeO in magnesiowüstite) may be described by

$$\log K = \log (a_{FeO}/a_{Fe}) - (1/2)\log fO_2^{exp} \quad , \tag{9}$$

where log fO_2^{exp} is the oxygen fugacity of the high-pressure experiment. The equilibrium constant for the reaction between pure Fe and pure FeO (which defines the IW buffer), with $a_{Fe} = 1$ and $a_{FeO} = 1$, reduces to

$$\log K = -1/2 \log fO_2^{IW} \quad , \tag{10}$$

where log fO_2 (IW) gives the oxygen fugacity of the Fe–FeO equilibrium under the P-T conditions of the experiment. The oxygen fugacity of the experiment may also be expressed relative to the IW-buffer curve

$$\log fO_2^{exp} = \log fO_2^{IW} - \Delta IW \quad , \tag{11}$$

where ΔIW is the difference between log fO_2^{IW} and the oxygen fugacity of the experiment (log fO_2^{exp}). Combining Eqns 9, 10, and 11 then gives

$$\log (a_{FeO}/a_{Fe}) - 1/2\,(\log fO_2^{IW} - \Delta IW) = -1/2 \log fO_2^{IW}$$

and thus

$$2 \log (a_{FeO}/a_{Fe}) = \Delta IW \quad , \tag{12}$$

where a_{FeO} and a_{Fe} are the activities of FeO and Fe in magnesiowüstite and metal, respectively. Inserting the respective activities of Fe and FeO in the product phases into Eqn 12 thus allows the oxygen fugacity to be determined relative to the Fe–FeO equilibrium.

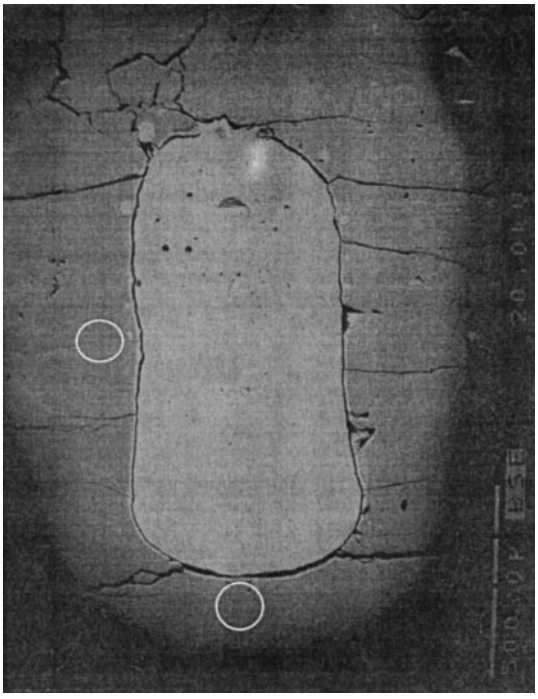

Fig. 1. Backscattered electron image of sample 1194 showing the quenched liquid metal (white) surrounded by the magnesiowüstite capsule (grey). The white circles at the side and the bottom of the sample show the areas where mössbauer spectra were taken. The Mössbauer spectrum shown in Fig. 3 has been taken at the side of the sample.

4. RESULTS AND DISCUSSION

4.1. Product Phases

Under the pressure–temperature conditions of the experiments (Table 2), the metal phase is always liquid. In the quenched samples, the metal consists of small oxide-rich "blobs" contained in a metal-rich matrix. These blobs are interpreted to form by exsolution during the quench (O'Neill et al., 1998; Gessmann and Rubie, 1998). During the experiments, Fe and other siderophile and light elements diffused into the MgO capsule material, thus forming magnesiowüstite solid solutions. A backscattered electron image of a typical sample (Fig. 1) shows the quenched liquid metal enclosed by the magnesiowüstite capsule. Detailed descriptions of the product phases and evidence for the extent of chemical equilibration are given in Gessmann and Rubie (1998). The attainment of equilibrium is documented by broad, flat Fe-concentration profiles (up to 250 μm long) which develop in the initially Fe-free MgO capsule wall adjacent to the liquid metal (Gessmann and Rubie, 1998).

Because the blobs in the quenched metal are interpreted to have formed by exsolution during the quench, the liquid metal composition under the conditions of each experiment has to be calculated by integrating the blob and metal–matrix compositions on the basis of their respective volume fractions (see Gessmann and Rubie, 1998). The distribution of element M between the liquid metal and magnesiowüstite is given by $D_M^{met/ox}$ ($D_M^{met/ox} = c_M^{met}/c_M^{ox}$; wt% basis), values of which are listed, together with uncertainties derived from error propagation, in Table 3.

4.2. Oxygen Fugacity Estimates

As described above, different oxygen fugacities were imposed on the sample by varying the silicon to oxygen ratio in the starting material. The oxygen fugacity for each experiment has been calculated using Eqn 12 and two different activity–composition models, as described below. The effectiveness of using different starting materials to vary the redox conditions in multianvil experiments is shown by Fig. 2 in which calculated oxygen fugacities are plotted as a function of the Si/O ratio of the starting material.

The use of Eqn 12 to calculate the oxygen fugacity, relative to that defined by the Fe–FeO equilibrium, requires knowledge of the activities of Fe in metal and FeO in magnesiowüstite. With $a_i^j = X_i^j \gamma_i^j$, the compositions X_i^j and the activity coefficients γ_i^j are needed for this calculation. Unfortunately, the activity coefficients γ_{Fe} for metal and γ_{FeO} for magnesiowüstite are not known at the pressures and temperature of the experi-

Table 3. Metal–magnesiowüstite distribution coefficients calculated from the integrated metal liquid (metal matrix and blob analysis integrated based on their respective volume fractions and the densities of the phases) and the magnesiowüstite electron microprobe analysis.

Experiment	log D_{Ni}	log D_{Co}	log D_{Mn}	log D_{Cr}	log D_V	log D_{Si}
1186	2.03 (.05)		−0.71 (.03)	−0.48 (.05)	−1.05 (.05)	0.44 (.08)
1194	1.74 (.08)		−0.91 (.13)	−0.86 (.12)	−1.12 (.11)	0.15 (.25)
1200	2.33 (.11)		−0.40 (.05)	−0.02 (.02)	−0.61 (.05)	1.40 (.08)
1203	2.65 (.35)		0.13 (.06)	0.54 (.06)	0.91 (.10)	2.26 (.10)
1210	1.83 (.04)		−0.84 (.09)	−0.72 (.11)	−1.13 (.08)	0.22 (.28)
1218	2.33 (.15)		−0.26 (.08)	0.07 (.08)	−0.50 (.19)	1.60 (.19)
1316	2.68 (.19)	2.32 (.22)	0.06 (.03)	0.48 (.02)	−0.06 (.09)	2.30 (.09)
1352	1.82 (.04)	1.36 (.02)	−0.83 (.07)	−0.72 (.09)	−1.08 (.09)	0.31 (.20)
1371	1.82 (.05)	1.33 (.06)	−0.88 (.10)	−0.76 (.16)	−1.12 (.17)	0.09 (.29)
1383	1.81 (.06)	1.34 (.04)	−0.80 (.05)	−0.69 (.07)	−1.00 (.11)	0.27 (.16)
1273	1.94 (.10)		−0.55 (.07)	−0.23 (.09)	−0.88 (.11)	0.72 (.07)
1275	1.84 (.05)		−0.55 (.11)	−0.23 (.06)	−0.89 (.10)	0.79 (.08)
1285	1.47 (.02)		−1.03 (.17)	−0.89 (.19)	−1.33 (.21)	0.01 (.15)
1320	2.17 (.10)	1.94 (.10)	0.00 (.04)	0.31 (.06)	−0.27 (.09)	2.06 (.15)
1334	2.10 (.13)	1.65 (.15)	−0.29 (.09)	0.07 (.09)	−0.48 (.15)	1.35 (.41)
1342	1.53 (.10)	1.11 (.10)	−1.19 (.11)	−0.91 (.11)	−1.40 (.29)	below D.L.

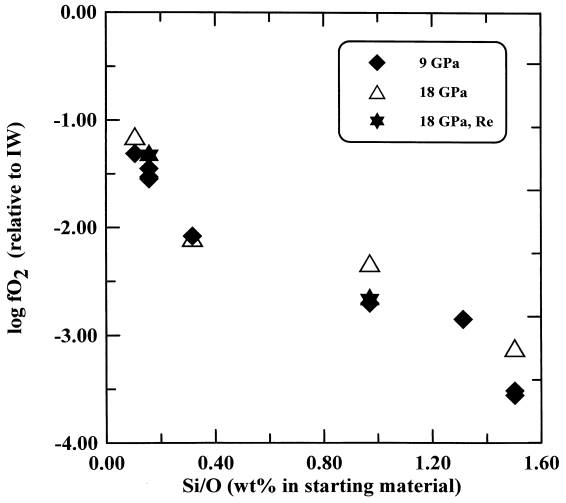

Fig. 2. Oxygen fugacity as a function of silicon to oxygen ratio (wt%) of the starting material. fO_2 has been calculated based on the Fe–FeO equilibrium determined in the quenched run products assuming ideal mixing in both phases. Changing the composition of the starting material enables a wide range of different oxygen fugacities to be imposed.

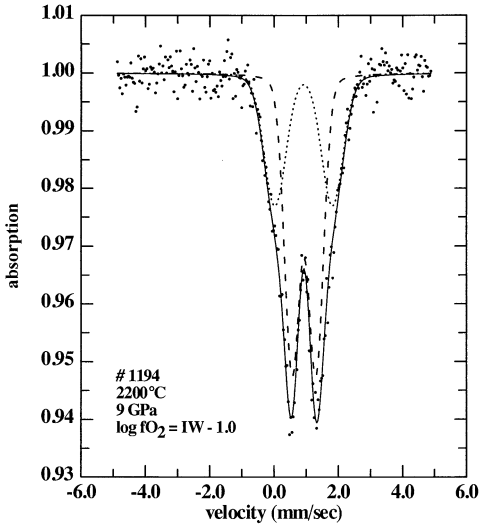

Fig. 3. Mössbauer spectrum of sample 1194 obtained from the area at the side of the sample shown in Fig. 1. The two symmetric subspectra indicate the absence of measurable amounts of ferric iron.

ments. Because activity coefficients are expected to approach unity with increasing temperature, the assumption that $a_i^j = X_i^j$ may be reasonable for the present experiments (although the effect of high pressure on mixing properties is not known). Substitution of the analyzed Fe and FeO contents (in mol%) of the product phases into Eqn 12 thus allows the oxygen fugacities to be estimated (Table 2, Fig. 2). Such estimates can also be made using activity coefficients of the respective components determined at 1 bar, as listed in Table 2. The 1 bar activity coefficients determined for liquid Fe–Ni metal (at 1873 K) by Rammensee and Fraser (1981) and those determined for magnesiowüstite (at 1050–1400 K) by Screčec et al. (1987) have been applied. In no case do the two estimates deviate from each other by more than 0.6 log bar units (Table 2) (see also Gessmann et al., 1997). The partitioning results discussed below suggest that the oxygen fugacities based on ideal mixing of Fe and FeO in the product phases are the better estimates. This would be consistent with the very high temperature (2200°C) of the experiments.

4.3. Mössbauer Spectroscopy

The oxygen fugacities calculated relative to the Fe–FeO equilibrium are listed together with the other experimental conditions in Table 2 and range from IW−1 to IW−3.5 (where IW denotes the fO_2 at the iron–wüstite buffer under the respective P–T conditions). It is unlikely that ferric iron is present in the run products at redox conditions below the iron–wüstite buffer. However, ferric iron was sometimes added to the starting material (as magnetite) and neglecting its presence in magnesiowüstite would clearly effect the reliability of the oxygen fugacity calculations. In order to test this possibility, a Mössbauer experiment was performed on one of the most oxidized samples to measure the ferric iron content of the run products.

The Mössbauer experiment was performed on sample #1194. The starting material for this sample contained 25 wt% Fe_3O_4; the calculated oxygen fugacity is ~1 log bar unit below the IW buffer, and this is one of the most oxidized experiments described here. Mössbauer spectra were collected from ~100 μm diameter regions of the magnesiowüstite capsule (see McCammon et al. (1991) for a description of the technique). Two areas were analyzed: one at the side and one at the bottom of the capsule wall (Figure 1). Both areas gave similar spectra (Fig. 3), and indicate no ferric iron within the detection limit ($Fe^{3+}/Fe_{total} < 2\%$, which corresponds to a detection limit of 0.17 wt% for sample #1194). This result suggests that the entire ferric iron of the starting material has been reduced to ferrous iron during the experiment. Therefore the possibility that ferric iron in magnesiowüstite has a significant effect on the oxygen fugacity estimates can be excluded.

4.4. Henry's Law Limits

The concentrations of Cr, Mn, and V in coexisting metal and magnesiowüstite vary between several 100 ppm and 2 wt%. Because of these low concentration levels it may be reasonable to assume that Henry's law is obeyed. In the case of other elements, Henry's law may not apply because of high concentrations (i.e., the activity coefficients may not be constant over the range of experimental conditions). The concentrations of Ni, Co, and Si in the liquid metal alloy, for instance, can be as high as several wt% (10–30 wt% in the case of Ni). However, other authors have provided evidence for constant activity coefficients, even at such high element concentration levels. Thibault and Walter (1995) presented evidence that the activity coefficients γ_{Co}^{met} and γ_{CoO}^{sil} do not change significantly with concentration in high pressure and high temperature liquid metal–liquid silicate partitioning experiments, even though

Henry's law might not be strictly obeyed. In the case of Ni, Pretorius and Muan (1992) showed in 1 bar experiments at 1400°C that γ_{NiO} remains constant up to several wt% NiO in silicate melt.

To further test if Henry's law is obeyed in the present experiments, results obtained under constant P–T–fO_2 conditions are compared. Because the experiments have not been specially designed to test for Henry's law, the number of data for each set of P, T, fO_2 conditions is small. Figure 4 shows the concentrations of elements in the metal plotted against their concentration in the oxide phase. Similar symbols denote element concentrations in experiments performed under the same P–T and redox (within 0.2 log bar units) conditions. Most of these data can be fitted by straight lines through the origin and are therefore consistent with Henry's law behavior.

4.5. Valence States

Metal–magnesiowüstite distribution coefficients for Ni, Co, Cr, V, Mn, and Si plotted as a function of oxygen fugacity (calculated assuming ideal activities of Fe in the metal and FeO in magnesiowüstite) are shown in Figs. 5–10. The slope of each regression line gives the valence of the respective element in magnesiowüstite according to Eqn 7. The two experiments performed with Re–foil capsules surrounding the MgO capsule (in which Fe–Ni–Re metal liquids are equilibrated with magnesiowüstite) at 18 GPa give results that are generally consistent with the trends defined by the other data. The results of these Re-bearing experiments have therefore been included in the linear regressions. However, deviations from the general trends are observed for the Mn and V distribution coefficients for one Re-bearing experiment (at high fO_2) and the valences for these elements have also been calculated omitting these results (Table 4). The data set for Co is relatively small because this element was not present in all starting materials (Table 1). The valences calculated from the slopes of the regression lines at constant pressure and temperature (Figs. 5–10) are given in Table 4. Valences based on oxygen fugacities calculated using 1 bar activity–composition relations (Rammensee and Fraser, 1981; Screčec et al., 1987) are also listed in Table 4 for comparison. The uncertainties of the valence states, based on the standard deviations of the regression line slopes, are generally less than ± 0.2 (Table 4).

The valences of Co, Mn, and V calculated from the slopes of the regression lines in Figs. 6–8 are $+1.95$, $+1.8$, and $+1.95$ at 9 GPa and $+1.82$, $+2.06$, and $+2.11$ at 18 GPa, respectively. Within error, these results indicate that these elements are divalent in magnesiowüstite, as expected. The calculated valences of Si ($+4.03$ and $+4.02$ at 9 and 18 GPa, respectively, see Fig. 10) are consistent with an oxidation state of $+4$ (Table 4). In contrast to these results significant deviations from expected valences are observed for the elements Ni and Cr (see discussion below). There are no indications for significant changes in valence state as a function of pressure for any of the elements over the investigated pressure range of 9–18 GPa, (Figs. 5–10).

The valences determined for Ni are $+1.65$ (± 0.04) and $+1.51$ (± 0.09) at 9 and 18 GPa, respectively and for Cr are $+2.44$ (± 0.06) and $+2.59$ (± 0.18) at 9 and 18 GPa, respectively (Table 4). Possible causes for the deviations from the expected valence states include: (i) erroneous oxygen fugacity estimates, (ii) the presence of mixed valence states, and (iii) nonideal mixing of the respective elements in one or both product phases.

Erroneous oxygen fugacity estimates would result if the assumption of ideal mixing of Fe in metal and FeO in the oxide is not valid. However, the fact that the valences determined for Co, Mn, V, and Si using the same oxygen fugacity estimates are consistent with the expected values argues against this possibility. The use of activity coefficients for Fe and FeO determined at 1 bar for the oxygen fugacity calculations (Table 4) results in significant deviations from expected valences not only for Ni and Cr, but also for Si. This suggests that the latter fO_2 estimates are not as good as those based on the assumption of ideal mixing of Fe in metal and FeO in the oxide phase. However, the possibility of nonideal behavior of Si canceling out errors in the fO_2 estimates cannot be excluded.

In the case of Cr the apparently high valence could indicate the presence of both Cr^{2+} and Cr^{3+} in magnesiowüstite under experimental conditions. Although the very high temperature of this study is expected to stabilize Cr^{2+}, the high pressures may help to stabilize Cr^{3+} (Li et al., 1995). However, the nearly linear trend shown in Fig. 9 argues against this possibility because the Cr^{2+}/Cr^{3+} ratio is likely to vary as a function of fO_2 at constant pressure and temperature; this should therefore result in a change in slope as a function of fO_2 in the plot of Fig. 9. Mixed valence states cannot explain the low valence obtained for Ni because they would require the presence of zero valent Ni in magnesiowüstite.

Despite the fact that the activity coefficients are expected to approach unity with increasing temperature, the deviations of the valences determined for Ni and Cr from $+2$ may indicate that the activity coefficients for these elements, γ_M^{met} and/or γ_{MO}^{mw}, are not constant, as required for Eqn 7 to be valid. One possibility is that nonideal mixing of Ni in the Fe–Ni alloy plays a role because of the large variation in the Ni content of this phase (Fig. 4). Rearranging Eqn 2, with γ_{Ni}^{met} as a variable and employing the 1 bar data of Rammensee and Fraser (1981) for Fe–Ni alloys gives almost identical results to those shown in Fig. 5. However, mixing may become less ideal at high pressure. In the case of magnesiowüstite, although the concentration of Ni is low ($\leq$1 wt%, Fig. 4), there is evidence that metal–oxide partition coefficients for Ni depend strongly on magnesiowüstite composition (Gessmann and Rubie, 1998). This would indicate that mixing of NiO in magnesiowüstite is nonideal and could therefore be a cause of the low valence estimate.

As for Ni, application of the 1 bar activity coefficients for Cr in Fe–Cr liquid alloys (Hultgren et al., 1973) results in negligible changes in the calculated valences and cannot therefore explain the results for Cr. To our knowledge activity–composition data for mixing of Cr in magnesiowüstite are not available.

In summary, the most likely cause of the deviations from expected valences for Ni and Cr are nonideal mixing in magnesiowüstite and/or liquid metal. However, the possibility of mixed valence states contributing to the results cannot be excluded.

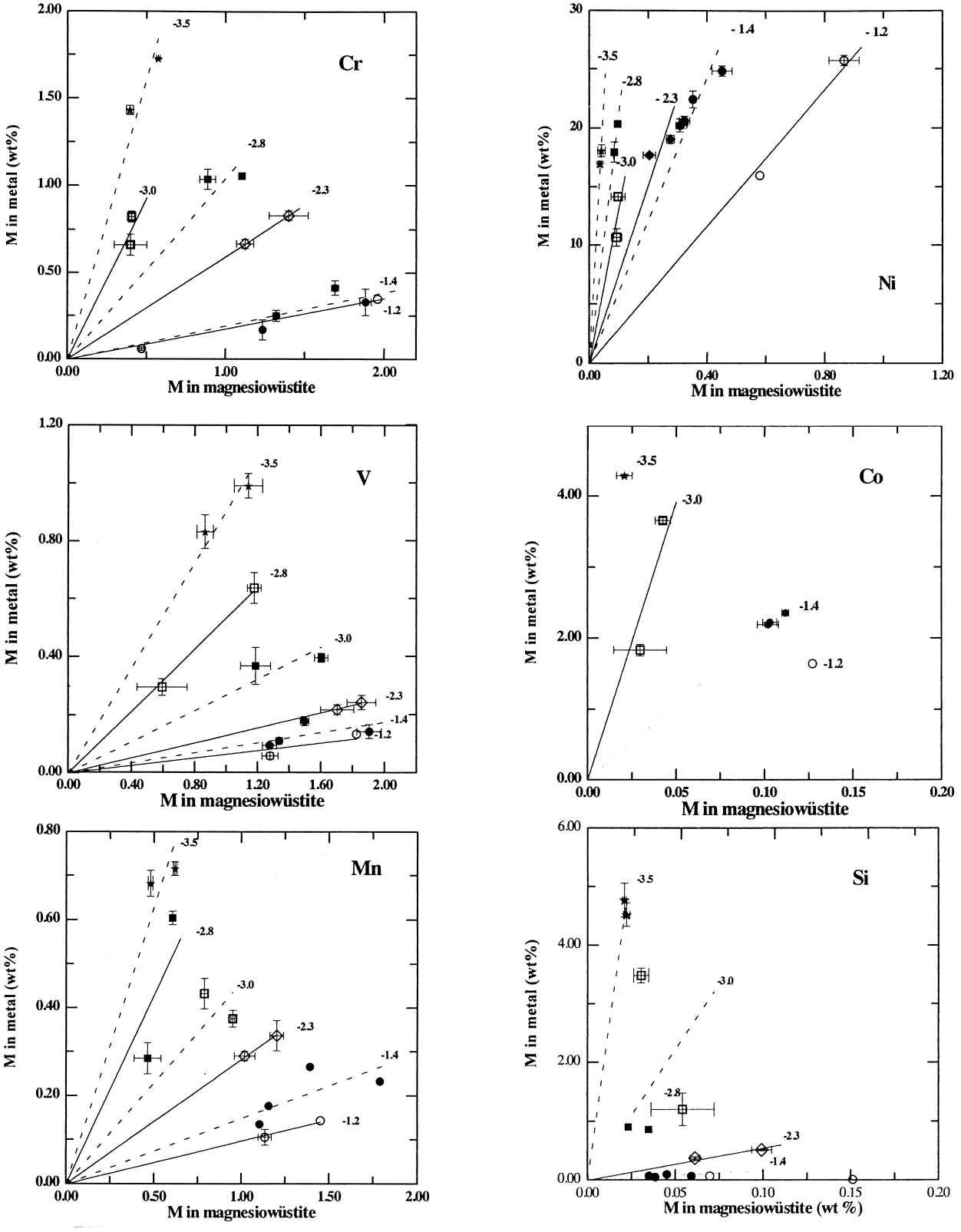

Fig. 4. Concentrations of Cr, V, Mn, Ni, Co, and Si in metal versus their concentrations in magnesiowüstite (wt%). Similar symbols represent fixed P, T, and fO_2 conditions. The lines are fitted through each set of symbols and the origin. Solid lines indicate 18 GPa data, broken lines denote 9 GPa experiments. The numbers give the calculated oxygen fugacity relative to the iron–wüstite buffer for each set of experimental conditions. Henry's law appears to be obeyed at the experimental conditions.

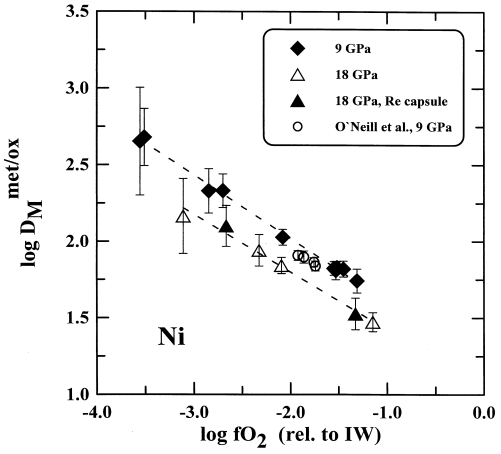

Fig. 5. Metal–magnesiowüstite distribution coefficients for Ni as a function of oxygen fugacity at 9 and 18 GPa and 2200°C. The slope of the regression lines corresponds to the valence of Ni in magnesiowüstite (regression coefficients R^2 are 0.9957 and 0.9916 for 9 and 18 GPa, respectively). Data of O'Neill et al. (1998) are shown for comparison.

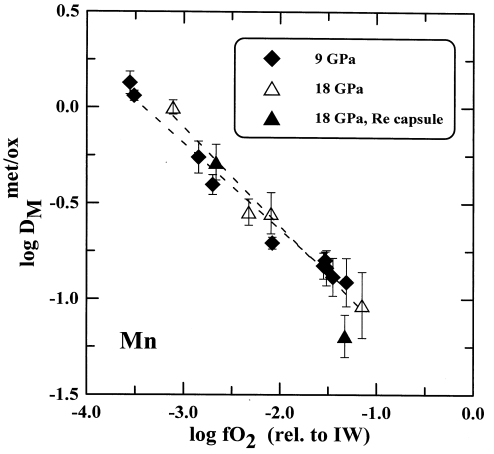

Fig. 7. Metal–magnesiowüstite distribution coefficients for Mn as a function of oxygen fugacity at 9 and 18 GPa and 2200°C. The slope of the regression lines corresponds to the valence of Mn in magnesiowüstite (regression coefficients R^2 are 0.98142 and 0.9773 for 9 and 18 GPa, respectively).

4.6. Comparison to Literature Data

There are few other existing data with which the present results can be compared. O'Neill et al. (1998) also investigated the partitioning of Ni, Co, and Cr between magnesiowüstite and liquid metal and their partitioning results are consistent with those of the present study at 9 GPa within error (Figs. 5, 6 and 9). They reported results that are consistent with Ni and Co being divalent and Cr being trivalent in magnesiowüstite. The differences between their results and those of the present study for Ni and Cr can be attributed to the narrow oxygen fugacity range of their experiments (<0.2 log bar units) compared with that of our study (~3 log bar units). The only other comparable high-pressure study is that of Thibault and Walter (1995) who studied partitioning of Ni and Co between silicate melt and liquid metal at 5 GPa. For Ni and Co in silicate melt, they reported valences of +2 and +2.1, respectively; however, the oxygen fugacity range of their experiments was also narrow (0.5–0.7 log bar units) and the number of experiments was small.

To our knowledge there are no other systematic high-pressure data available to constrain the valence states of Mn, Cr, and V in metal–silicate or metal–oxide systems. Drake et al. (1989) reported valences for Mn, Cr, and V in silicate melt based on metal–silicate partitioning experiments performed at 1 bar and 1260°C over an oxygen fugacity range comparable to that of the present study. Their results indicate that Cr and Mn are divalent and V is trivalent in silicate liquid. The most likely explanation for the differences between their results and those of the present study is that the valence of V (and possibly that

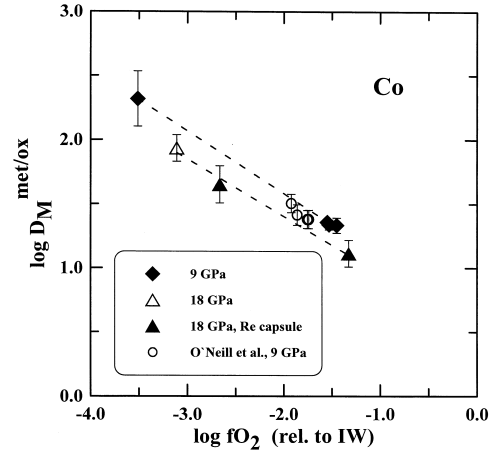

Fig. 6. Metal–magnesiowüstite distribution coefficients for Co as a function of oxygen fugacity at 9 and 18 GPa and 2200°C. The slope of the regression lines corresponds to the valence of Co in magnesiowüstite (regression coefficients R^2 are 0.9992 and 0.9936 for 9 and 18 GPa, respectively). Data of O'Neill et al. (1998) are shown for comparison.

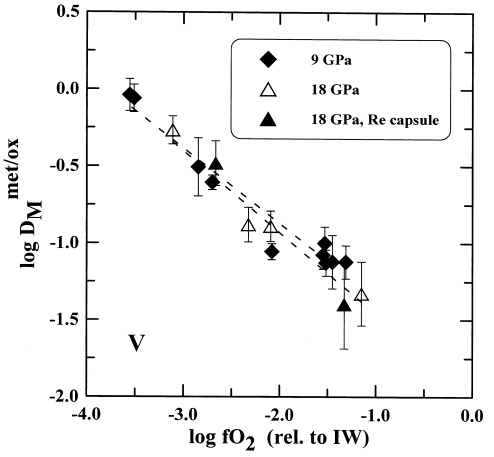

Fig. 8. Metal–magnesiowüstite distribution coefficients for V as a function of oxygen fugacity at 9 and 18 GPa and 2200°C. The slope of the regression lines corresponds to the valence of V in magnesiowüstite (regression coefficients R^2 are 0.95013 and 0.9589 for 9 and 18 GPa, respectively).

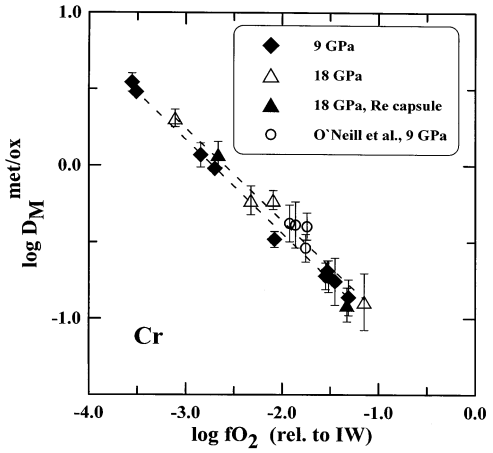

Fig. 9. Metal–magnesiowüstite distribution coefficients for Cr as a function of oxygen fugacity at 9 and 18 GPa and 2200°C. The slope of the regression lines corresponds to the valence of Cr in magnesiowüstite (regression coefficients R^2 are 0.9956 and 0.98568 for 9 and 18 GPa, respectively). Data of O'Neill et al. (1998) are shown for comparison.

of Cr) is different in magnesiowüstite and silicate liquid. It is critical to be aware of such differences when extrapolating partitioning data to different oxygen fugacities.

4.6. Consequences for Extrapolation of Element Partitioning Data

The determined divalent oxidation states for Co, Mn, V, and the 4+ valence of Si are as expected. Therefore, assuming these formal valences for a fO_2 normalization and the extrapolation of element partitioning data is likely to provide reliable results. In the case of Ni and Cr, however, omitting the likely nonideal mixing properties will affect the extrapolation of high-pressure element partitioning data. The exact consequences are difficult to assess without the detailed knowledge of the activity–composition relations for the respective phases. It is clear, however, that ignoring nonideal mixing properties will increase the scatter of data which have been normalized for oxygen fugacity (e.g., normalized to D_{Fe}), at least if the experiments cover a relatively broad range of redox conditions.

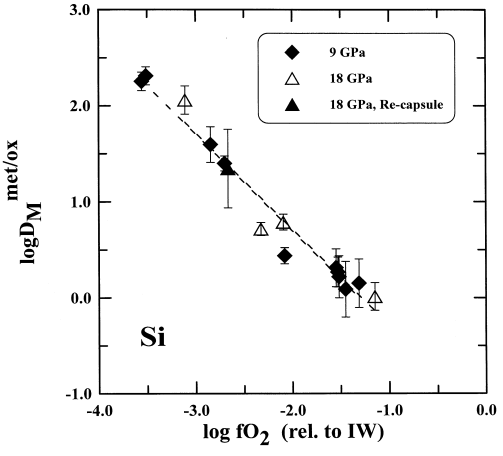

Fig. 10. Metal–magnesiowüstite distribution coefficients for Si as a function of oxygen fugacity at 9 and 18 GPa and 2200°C. The slope of the regression lines corresponds to the valence of Si in magnesiowüstite (regression coefficients R^2 are 0.97813 and 0.9166 for 9 and 18 GPa, respectively).

For the present experiments, the magnitude of errors that would result if data are extrapolated over an fO_2 range of 3 log bar units assuming ideal mixing and valances of 2+ can be estimated. For Ni, the error in the distribution coefficients could be as much as 0.25 log units. For example, at low oxygen fugacities a value for $D_{Ni} = 790$ would be obtained instead of 460. For Cr the error would be on the order of 0.4 log units. Such errors could significantly affect the comparisons of data sets obtained under different conditions of P, T and fO_2.

4.7. Partitioning Behavior of Cr, V, and Mn

One explanation for the low abundances of Cr, V, and Mn in the Earth's mantle is that these elements were siderophile under conditions of core formation, possibly because of high-pressure, high temperature and/or low oxygen fugacities. The effects of high pressure on the partitioning behavior of Ni and Co in various metal–oxide and metal–silicate systems are well documented (Urakawa, 1991; Gessmann et al., 1995; Thibault and Walter, 1995; Li and Agee, 1996; O'Neill et al., 1998, see also Figs. 5 and 6). According to the present results, however, the distribution coefficients for Mn, Cr, and V are similar at 9 and 18 GPa (Figs. 7–9), thus suggesting that the dependence of partitioning on pressure is relatively weak for these elements.

The high-pressure distribution coefficients for Cr, V, and Mn, determined at 9–18 GPa and 2200°C, indicate that all three elements become siderophile (i.e., $D_M > 1$) below oxygen fugacities of IW −2.7 to IW −3.7 (Figs. 7–9). These conditions are relatively reducing compared to those that were likely during core formation (e.g., Righter et al., 1997; Li and Agee, 1996). However, it has been shown that the D_{Fe}-normalized distribution coefficients for Cr, V, and Mn increase with increasing temperature at constant pressure (Gessmann and Rubie, 1998). Therefore, at temperatures higher than 2200°C the change from lithophile to siderophile behavior should occur under more oxidizing conditions. Thus, it may still be possible to explain the present abundances of Cr, V, and Mn in the Earth's mantle through a single-stage equilibrium model for core formation. This would be consistent with partitioning data for Ni and Co in metal–oxide and metal–silicate systems, which suggest that core formation occurred by the segregation of metal at pressures of above 25 GPa and temperatures above 2200°C (Gessmann et al. 1995; Li and Agee, 1996; Righter et al., 1997; Gessmann and Rubie, 1998). This conclusion, however, is only valid if pressure has little effect on the metal–oxide and metal–silicate distribution coefficients of Cr, V, and Mn, which has not yet been investigated.

5. CONCLUDING REMARKS

We have demonstrated that the variation of the Si/O ratio in the starting material can impose a wide range of oxygen fugacities in high-pressure metal–oxide partitioning experiments. The comparison of results derived with different oxygen fu-

Table 4. Slopes of regression lines in Figs. 5–10 and the corresponding valences calculated according to Eqn 7. Temperature in all experiments was 2200°C, the oxygen fugacity ranges from IW −1 to IW −3.5.

Element	Pressure	Slope (ideal model)*	Calc. valence (ideal model)*	Slope (nonideal model)*	Calc. valence (nonideal model)*
Ni	9	−0.414 (±0.01)	+1.66 (±0.04)	−0.458 (±0.01)	+1.83 (±0.04)
Ni	18	−0.377 (±0.02)	+1.51 (±0.09)	−0.399 (±0.033)	+1.60 (±0.13)
Co	9	−0.487 (±0.01)	+1.95 (±0.04)	−0.538 (±0.01)	+2.15 (±0.03)
Co	18	−0.455 (±0.04)	+1.82 (±0.15)	−0.519 (±0.03)	+2.08 (±0.01)
Mn	9	−0.449 (±0.02)	+1.78 (±0.09)	−0.500 (±0.02)	+2.00 (±0.09)
Mn	18	−0.575 (±0.04)	+2.30 (±0.17)	−0.648 (±0.06)	+2.59 (±0.26)
	18[a]	−0.516 (±0.06)	+2.06 (±0.22)	−0.580 (±0.06)	+2.32 (±0.26)
Cr	9	−0.611 (±0.02)	+2.44 (±0.06)	−0.675 (±0.05)	+2.70 (±0.20)
Cr	18	−0.648 (±0.05)	+2.59 (±0.18)	−0.727 (±0.05)	+2.91 (±0.20)
V	9	−0.488 (±0.04)	+1.95 (±0.16)	−0.539 (±0.04)	+2.16 (±0.17)
V	18	−0.577 (±0.06)	+2.31 (±0.23)	−0.646 (±0.07)	+2.58 (±0.27)
	18[a]	−0.528 (±0.08)	+2.11 (±0.31)	−0.595 (±0.09)	+2.38 (±0.34)
Si	9	−1.01 (±0.05)	+4.03 (±0.21)	−1.11 (±0.06)	+4.45 (±0.23)
Si	18	−1.01 (±0.17)	+4.02 (±0.7)	−1.14 (±0.19)	+4.57 (±0.76)

* Ideal and non-ideal models refer to oxygen fugacities calculated assuming ideal activities of FeO in magnesiowüstite and Fe in liquid metal and nonideal mixing properties as determined at 1 bar, respectively.

[a] For comparison: slope of regression lines omitting the Re-bearing experiments.

gacity estimates (i.e., assuming ideal mixing properties or employing 1 bar activity data for the Fe–FeO equilibrium) indicates that mixing of Fe in both liquid metal and magnesiowüstite is nearly ideal at high pressure and temperature. It is concluded, that metal–magnesiowüstite assemblages can provide reliable redox estimates for high-pressure experiments.

There are no indications for notable changes of the oxidation state of the investigated elements as a function of pressure. The calculated valences (assuming ideal mixing of the investigated elements in both metal and oxide) at 9 and 18 GPa and 2200°C are 2+ for Co, Mn, and V and 4+ for Si. However, the calculated oxidation states for Ni and Cr deviate significantly from the expected values. The apparent mixed valences for Ni and Cr are probably due to nonideal mixing properties in one or both of the phases present. The consequences of neglecting such nonideal mixing properties for Cr and Ni when extrapolating data from high-pressure element partitioning studies may be significant.

The elements Cr, V, and Mn become siderophile (i.e., $D_M^{met/ox} > 1$) at high pressure and high temperature below oxygen fugacities of IW −2.7 to IW −3.7. The change towards siderophile behavior will shift towards more oxidizing conditions with increasing temperature (Gessmann and Rubie, 1998). The depletion of Cr, Mn, and V in the Earth's mantle may therefore be at least partly a consequence of siderophile behavior at high pressure and temperature.

Acknowledgments—We thank Hubert Schulze and Oskar Leitner for very careful sample preparation and Detlef Krausse for assistance with microprobe analyses. We gratefully acknowledge discussions with Fritz Seifert and other colleagues from the Bayerisches Geoinstitut and the Deutsche Forschungsgemeinschaft (DFG) priority program on "Element Partitioning". The comments of two anonymous reviewers were greatly appreciated. This study was funded by DFG Grant No. RU 437/3-2 and by the EU "Human Capital and Mobility - Access to Large Scale Facilities" program (Contract No. ERBCHGECT940053).

REFERENCES

Borisov A. and Palme H. (1995) The solubility of Iridium in silicate melts: New data from experiments with $Ir_{10}Pt_{90}$ alloys. *Geochim. Cosmochim. Acta* **59,** 481–485.

Brümmer O. (1977) *Mikroanalyse mit Elektronen- und Ionensonden*. VEB Deutscher Verlag fuer Grundstoffindustrie.

Burns R. G. (1993) Mineralogical Applications of Crystal Field Theory. In *Cambridge Topics in Mineral Physics and Chemistry* (eds. A. Putnis, R. C. Liebermann). Chapter 9, p. 353–395.

Canil D. (1991) Experimental evidence for the exsolution of cratonic peridotite from a high-temperature harzburgite. *Earth Planet. Sci. Lett.* **106,** 64–72.

Drake M. J., Newsom C. J., and Capobianco C. J. (1989) V, Cr and Mn in the Earth, Moon, EPB, and SPB and the origin of the Moon: Experimental Studies. *Geochim. Cosmochim. Acta* **53,** 2101–2111.

Ertel W. (1996) Betsimmung des Löslichkeitsverhaltens und der Metall-Silikat-Verteilungskoeffizienten der siderophilen Elemente (Ni, W, Ir, Pt, Rh und Re) in einer haplobasatlitschen Schmelze bei hohen Temperaturen. PhD thesis, Univ. Bayreuth. 154 p.

Ertel W., O'Neill H. St. C., Dingwell D. B., and Spettel B. (1996) Solubility of tungsten in a haplobasaltic melt as a function of temperature and oxygen fugacity. *Geochim. Cosmochim. Acta* **60,** 1171–1180.

Gessmann C. K. and Rubie D. C. (1996) Valence states of siderophile elements at high pressure and temperature - experiments, results, restrictions. V. M. Goldschmidt Conf. 1996. *J. Conf. Abstracts* **1,** 202–203.

Gessmann C. K. and Rubie D. C. (1998) The effect of temperature on siderophile element partitioning at 9 GPa and constraints on formation of the Earth's core. *Geochim. Cosmochim. Acta* **62,** 867–882.

Gessmann C. K., McCammon C., and Rubie D. C. (1997) Oxygen fugacity constraints in unbuffered multianvil high-pressure experiments. *Terra Nova* **9,** 434 (abstr.).

Gessmann C. K., Rubie D. C., and O'Neill H. St. (1995) The effects of pressure, temperature and oxygen fugacity on element partitioning between magnesiowüstite and liquid metal: Implications for the formation of the Earth's core. *Euro. J. Minero.* **7,** 70.

Hillgren V. J. (1991) Partitioning behavior of Ni, Co, Mo and W between basaltic liquid and Ni-rich metal: Implications for the origin of the Moon and Lunar core formation. *Geophys. Res. Lett.* **18,** 2077–2080.

Holzheid A., Borisov A., and Palme H. (1994) The effect of oxygen fugacity and temperature on solubilities of Nickel, Cobalt, and Molybdenum in silicate melts. *Geochim. Cosmochim. Acta* **58,** 1975–1981.

Hultgren R., Desai P. D., Hawkins D. T., Gleiser M., and Kelley K. K. (1973) Selected values of the thermodynamic properties of binary alloys. *American Society for Metals*. Book, 1435 p. Metals Park, Ohio.

Ito E., Takahashi E., and Matsui Y. (1984) The mineralogy and chemistry of the lower mantle: An implication of the ultrahigh-pressure phase relations in the system MgO–FeO–SiO_2. *Earth Planet. Sci. Lett.* **67,** 238–248.

Jones H. J. and Drake M. H. (1986) Geochemical constraints on core formation in the Earth. *Nature* **322,** 221–228.

Li J. and Agee C. B. (1996) Geochemistry of mantle-core formation at high pressure. *Nature* **381,** 686–689.

Li J-P, O'Neill H. St. C., and Seifert F. (1995) Subsolidus phase relations in the system MgO–SiO_2–Cr-O in equilibrium with metallic Cr, and their significance for the petrochemistry of chromium. *J. Petrology* **36,** 107–132.

Liebermann R. C. and Wang W. (1992) Characterization of sample environment in an uniaxial split-sphere apparatus. In *High Pressure Research: Application to Earth and Planetary Sciences*. (eds. Y. Syono and M. H. Manghnani), pp. 19–31. Terrapub.

Luth R. W. (1993) Measurement and control of intensive parameters in experiments at high pressure in solid media apparatus. In *Experiments at High Pressure and Applications to the Earth's Mantle. Short Course Handbook* (ed. R. W. Luth), Vol. 21.

McCammon C. A., Chaskar V., and Richards G. G. (1991) A technique for spatially resolved Mössbauer spectroscopy applied to quenched metallurgical slags. *Meas. Sci. Technol.* **2,** 657–662.

O'Neill H. St. C., Canil C., and Rubie D. C. (1998) Metal-oxide equilibria to 2500°C and 25 GPa: Implications for core formation and the light component in the Earth's core. *J. Geophys. Res.* **103,** 12,239–12,260.

O'Neill H. St. C., Dingwell D. B., Borisov A., Spettel B., and Palme H. (1995) Experimental petrochemistry of some highly siderophile elements at high temperatures, and some implications for core formation and the mantle's early history. *Chem. Geology* **120,** 255–273.

Pretorius E. B. and Muan A. (1992) Activity of Ni (II) oxide in silicate melts. *J. Am. Ceram. Soc.* **75,** 1490–1496.

Rammensee W. and Fraser D. G. (1981) Activities in solid and liquid Fe–Ni and Fe–Co alloys determined by Knudsen cell mass spectrometry. *Ber. Bunsenges. Phys. Chem.* **85,** 588–592.

Ramsden A. R. and French D. H. (1990) Routine trace-element capabilities of electron-microprobe analysis in mineralogical investigations: an empirical evaluation of performance using spectrochemical standard glasses. *Can. Mineralogist* **28,** 171–180.

Righter K., Drake M. J., and Yaxley G. (1997) Prediction of siderophile element metal/silicate partition coefficients to 20 GPa and 2800°C: The effects of pressure, temperature, oxygen fugacity and silicate and metallic melt compositions. *Phys. Earth Planet. Interiors* **100,** 115–134.

Ringwood A. E. (1966) The chemical composition and origin of the earth. In *Advances in Earth Sciences*. (ed. D. M. Hurley) pp. 287–356, MIT Press.

Rubie D. C., Karato S., Yan H., and O'Neill H. St. C. (1993a) Low differential stress and controlled chemical environment in multianvil high-pressure experiments. *Phys. Chem. Minerals* **20,** 315–322.

Rubie D. C., Ross II C. R., Caroll M. R., and Elphick S. C. (1993b) Oxygen self-diffusion in $Na_2Si_4O_9$ liquid up to 10 GPa and estimation of high-pressure melt viscosities. *American Mineralogist* **78,** 574.

Screčec I., Ender A., Woermann E., Gans W., Jacobsson E., Erikssom G., and Rosén E. (1987) Activity-composition relations of the magnesiowüstite solid solution series in equilibrium with metallic iron in the temperature range 1050–1400 K. *Phys. Chem. Minerals* **14,** 492–498.

Thibault Y. and Water M. J. (1995) The influence of pressure and temperature on the metal-silicate partition coefficients of nickel and cobalt in a model C1 chondrite and implications for metal segregation in a deep magma ocean. *Geochim. Cosmochim. Acta* **59,** 991–1002.

Urakawa S. (1991) Partitioning of Ni between magnesiowüstite and metal at high pressure: implications for core-mantle equilibrium. *Earth Planet. Sci. Lett.* **105,** 293–313.